

BULK IMAGE EFFECTS OF PHOTORESIST IN THREE-DIMENSIONAL PROFILE SIMULATION

Tatsumi ISHIZUKA

Fuji Research Institute Corporation
3-2-12, Kaigan, Minato-ku, Tokyo 108, JAPAN

Abstract: 3D bulk image effects in high-NA lens lithography are studied through 3D exposure and development simulations by applying a Mack model to the 3D exposure process.

1. INTRODUCTION

Extensive research has been carried out on lithography because it is essential technique by which to miniaturize semiconductor integrated circuits. In particular, photolithography has been widely used in an effort to improve the resolution property for reason of its industrial refinement and productivity. The resolution of $0.3 \mu\text{m}$ is required to realize the next generation, 64-megabit dynamic random access memories. To achieve this resolution, imaging systems with high numerical aperture (NA) have been proposed. The high-NA imaging systems have become crucial for high-resolution photolithography as the feature sizes of ultra large scale integration (ULSI) devices are continuously being scaled down. In general, the increase of NA for lens systems improves the resolution capability of an exposure system, while it brings about decrease in the depth of focus. Therefore, it is an urgent problem to exactly evaluate the focus effects on fine-line photolithography by means of numerical simulation. Asymmetry effects with respect to the focal plane (bulk image effects) have not been incorporated in the light intensity calculation at the photoresist surfaces. In order to simulate the bulk image effects exactly, C.A. Mack has proposed a model [1] (Mack model) by extending a vertical propagation model (VP model) adopted in SAMPLE [2] or other conventional simulators, and applied it to the two-dimensional (2D) simulation of photoresist cross-sectional features [2]. However, in the submicron region it is difficult to make appropriate estimations of photoresist profiles by using the simulators for 2D cross sections because the 2D simulation neglects the edge effects due to aerial image distribution [3]. Three-dimensional (3D) development simulations have been developed [3-8]. For 3D topography calculation, we have developed a new algorithm called the network method, which automatically avoids singular loops during the calculation and enables us to make a stable and accurate calculation of complicated 3D photoresist images [9-10]. The network method is applied in this work.

In this paper, the computational methods of the 3D exposure and the 3D development simulation are described in section 2; 3D bulk image effects in high-NA lens lithography are studied through 3D exposure and development simulations applying the Mack model to the 3D exposure process in section 3; and the result of analysis is summarized in section 4.

2. COMPUTATIONAL METHODS

2.1 3D aerial image inside photoresist

In reduction projection lithography, exposure occurs through a reticle (mask) set between an optical source and a photoresist film as shown in Fig.1. In the image space of the optical projection system, photoresist may be placed as semi-infinite refractive medium. As shown in Fig. 2, the light intensity on the z' plane in the photoresist is equivalent to that on the z plane in air [1],[11]. The relationship between z and z' is given by

$$z = R + z_0 + z'/n', \quad (1)$$

where R is the radius of the exit pupil, z_0 is the distance between the resist surface and the Gaussian image plane, z' is the depth into the photoresist layer, and n' is the resist refractive index. z is exactly redefined as the distance between the exit pupil and the image plane scaled in air. As a result, the 3D aerial image problem in the photoresist reduces to 2D calculation. The 2D aerial image calculation here is based on the method proposed by Yeung [12]. In this method, an illumination source is divided into a number of mutually incoherent point sources, and the image intensity due to partial coherent illumination is calculated by summing the coherent images formed by each source element. The image intensity $I_z(x, y)$ on the image plane is written in the following form:

$$I_z(x, y) = \frac{\sum_i |A_i| \cdot \iint \mathcal{F}(f - p_i/\lambda, g - q_i/\lambda) \cdot \mathcal{K}(f, g) \cdot \exp\{2\pi j(f \cdot x + g \cdot y)\} df dg}{\sum_i |A_i|^2}. \quad (2)$$

In eq. 2, $\mathcal{F}(f, g)$ is the Fourier transform of the amplitude transmittance at mask $F(x, y)$, f and g are spatial frequencies, λ is the wavelength of illumination light, (p_i, q_i) is the unit vector described as the direction cosine of illumination light corresponding to the i -th source element with amplitude A_i , and $j^2 = -1$. $\mathcal{K}(f, g)$ is the Fourier transform of the coherent transfer function related to the pupil function, $P(x, y)$, of the projection lens which can be written as follows:

$$\mathcal{K}(f, g) = P(-\lambda \cdot z \cdot f, -\lambda \cdot z \cdot g) \cdot \exp\{2\pi j \cdot W(-\lambda \cdot z \cdot f, -\lambda \cdot z \cdot g)/\lambda\}, \quad (3)$$

where $W(x, y)$ represents the wavefront aberration.

2.2 Exposure calculation

According to the previous approach, the image intensity $I(x, y, z')$ inside the resist is equal to $I_z(x, y)$ if the resist is of semi-infinite thickness. Independent of the above discussion, we can obtain the one-dimensional standing wave interference pattern $V_{x,y}(z', t)$ due to the complex refractive indices $n_{x,y}(z', t)$ inside the resist and the underlayers, assuming that the exposed light is normally incident into the resist [2]. In the resist layer, $n_{x,y}(z', t)$ is expressed as

$$n_{x,y}(z', t) = n' - j \cdot n''_{x,y}(z', t). \quad (4)$$

The imaginary part of $n_{x,y}(z', t)$, the extinction coefficient $n''_{x,y}(z, t)$, is varied as exposed time. The extinction coefficient $n''_{x,y}(z, t)$ can be calculated using the photosensitizer concentration $M(x, y, z', t)$ [13].

$$n''_{x,y}(z', t) = (\lambda/4\pi) \cdot \{A \cdot M(x, y, z', t) + B\}, \quad (5)$$

where A and B are light absorption constants given by Dill et al.'s model [13]. The 3D aerial image intensity $I_D(x, y, z', t)$ inside the resist with the standing wave effect can be written as

$$I_D(x, y, z', t) = I(x, y, z') \cdot V_{x,y}(z', t). \quad (6)$$

Equation 6 constitutes the principal relation of the Mack model, which separates the effects of defocus and interference [1]. Using the light intensity $I_D(x, y, z')$, we express the bleaching reaction in the resist as

$$\partial M(x, y, z', t)/\partial t = -I_D(x, y, z', t) \cdot M(x, y, z', t), \quad (7)$$

where C is the reaction rate constant [13].

When I_D and M are given at position (x, y, z') and exposed time t , M and n'' can be calculated at time $t + dt$ using eqs. 5 and 7. The complex refractive index n at time $t + dt$ affects the standing wave interference V at this time step and I_D is obtained by eq. 6. This calculation loop has been made to the end of exposure time.

2.3 Topography calculation

A newly developed network method [9-10] is applied to the 3D photoresist development simulation in this work. The idea of the network method is as follows: A resist layer is divided into cubic elements called a unit U_{ijk} and the unit is more divided into six tetrahedrons called a cell C_{ijkl} . The ensemble of all tetrahedrons' edge lines L_{ijkm} may be called the network. In Fig. 3 the cell decomposition of the unit U_{ijk} and the relationship of vertices P_{ijk} and edges L_{ijkl} in the unit U_{ijk} are shown. The advance of development is expressed by the movement of points $\vec{Q}(t)$ on the network which define the developed photoresist surface, and t is development time. The development rate of each vertex is calculated beforehand. The development rate on the edge line is linearly interpolated by rates of two vertices which define the edge line. The one-dimensional solution of the development time and the position is described [9] in the appendix, which is applied to the movement of the point on the network. We introduce the development index $I(P)$ of vertex P , the development direction index $K(L)$ of edge L , the edge vector $\vec{E}(L)$ of edge L , the development fraction $A(L)$ of edge L and the parameter q of development fineness. $I(P)$ is 0 or 1 if vertex P has been developed or has not been developed yet, respectively. $K(L)$ is -1, 0 or 1 defined as

$$K(L) = I(\vec{P}_1) - I(\vec{P}_2), \quad (8)$$

where \vec{P}_1 and \vec{P}_2 are two vertices of the edge L . If $K(L)$ is equal to 0, there is no \vec{Q} on L . Then, there is unique \vec{Q} on edge lines if it exists. Consequently, there exists no singular loop. The edge vector $\vec{E}(L)$ is defined as

$$\vec{E}(L) = K(L) \cdot (\vec{P}_2 - \vec{P}_1), \quad (9)$$

where \vec{P}_1 and \vec{P}_2 are the position vectors of the edge line. The edge vector $\vec{E}(L)$ has same length as edge line L , and the direction of the vector equals the direction of development. The development fraction $A(L)$ varies from 0 to 1 and is expressed as

$$A(L) = 1 - (\text{developed length of } L) / (\text{length of } L). \quad (10)$$

The parameter q of development fineness varies from 0.5 to less than 1.0. If the condition that $A(L)$ is less than $(1 - q)$ is satisfied, $I(\vec{P}_2)$ or $I(\vec{P}_1)$ is changed from 1 to 0 and edge line L has been developed. The interface vector \vec{W}_F is defined as shown in Fig. 4(a). The directions of normal vectors \vec{W}_{ij} for all planes spanned by vectors \vec{W}_F which contain the point $P = \vec{Q}(t)$ on edge L are selected as follows:

$$\vec{W}'_{ij} = \vec{W}_{F_i} \times \vec{W}_{F_j}, \quad (11)$$

$$\vec{W}_{ij} = \text{sign}(1, (\vec{E}(L) \cdot \vec{W}'_{ij})) \cdot \vec{W}'_{ij}, \quad (12)$$

where $\text{sign}(a, b)$ is 1 or -1 if the sign of a equals the sign of b or not, respectively. The direction of development at P is

$$\vec{W}(P) = \frac{\sum \vec{W}_{ij}}{|\sum \vec{W}_{ij}|}. \quad (13)$$

The development rate $r(P)$ at P on L is evaluated as

$$r(P) = \frac{q \cdot [v(\vec{P}_2) + \{v(\vec{P}_1) - v(\vec{P}_2)\} \cdot A(L)] \cdot |\vec{E}(L)| \cdot |\vec{W}(P)|}{|(\vec{E}(L) \cdot \vec{W}(P))|}, \quad (14)$$

where $v(\vec{P}_i)$ is the development rate on the vertex \vec{P}_i . These relations are shown in Fig. 4(b) and (c). In the initial state, all $I(P)$ of vertex P on the resist surface are zero. The advance of $\vec{Q}(t)$ is done in time step dt which is determined by minimum dt of every $\vec{Q}(t)$ to reach the vertex. The time to reach the vertex is evaluated by the equation in the appendix.

In Fig. 5, calculated profiles are shown. The strong standing wave effect in photoresist on a flat substrate has been successfully simulated.

3. BULK IMAGE EFFECTS

The resolution R in photolithography is given from the optical diffraction theory as follows:

$$R = K_1 \cdot (\lambda / \text{NA}), \quad (15)$$

where NA is the numerical aperture of the projection lens and λ is the wavelength of exposure light. Theoretically, the value of K_1 is 0.61. However, the value equal to or above 0.61 is empirically adopted when the total performance of the lithography process including development is considered. In this case, K_1 is an empirical constant, and is called the process coefficient. The resolution R represents a linewidth which can be resolved in actual lithography processes. Assuming that K_1 is 0.61 for the i-line ($\lambda = 0.365 \mu\text{m}$)

edge vector $\vec{E}(L)$ has same direction of development. Expressed as

$$\text{of } L). \quad (10)$$

than 1.0. If the condition changed from 1 to 0 and edge is shown in Fig. 4(a). The vectors \vec{W}_F which contain the

$$(11)$$

$$(12)$$

or not, respectively. The

$$(13)$$

$$\text{of } |\vec{W}(P)|, \quad (14)$$

relations are shown in Fig. The resist surface are zero. and by minimum dt of every evaluated by the equation in

ing wave effect in photoresist.

raction theory as follows:

$$(15)$$

and λ is the wavelength of over, the value equal to or of the lithography process ical constant, and is called which can be resolved in the i-line ($\lambda = 0.365 \mu m$)

reduction projection exposure system with a 0.42 NA lens, we obtain $R=0.52 \mu m$. The depth of focus D_f , which is very important in actual device fabrication processes, is expressed by the following equation:

$$D_f = 0.5 \cdot (\lambda/NA^2). \quad (16)$$

D_f becomes $1 \mu m$ assuming that λ is $0.365 \mu m$ and NA is 0.42. If we increase this NA value to improve the resolution of the exposure system, the depth of focus decreases rapidly as predicted from eq. 16, and it is an urgent problem to exactly estimate the focus effects when D_f is smaller than the step height on the device surfaces. The result of development simulation by changing NA and defocus, which means z_0 in eq. 1 is shown in Fig. 6. The calculation conditions were assumed as follows: The mask pattern was $0.6 \mu m \times 0.6 \mu m$ (development simulation was carried out for a quarter of the pattern area). The i-line light was irradiated from a light source with a coherence factor of $\sigma = 0.5$. Photoresist thickness was $1.2 \mu m$ and the substrate was bare silicon. Dill et al.'s photobleaching parameters [13] A , B , and C were 0.52, 0.062, and 0.018, respectively [3], and the development parameters [13] E_1 , E_2 , and E_3 were 8.09, -5.32, and -0.01, respectively [3]. The exposure dose was 72 mJ/cm^2 . Figure 6 shows that change in defocus (+ or -) causes significant difference in the developed profiles when NA is high. Computed change in the critical dimension is also shown in Fig. 7 for varied exposure doses. The results clearly indicate an asymmetric profile with respect to the focal plane, and the focus latitude can be estimated from Fig. 7.

4. CONCLUSIONS

The resolution performance of an i-line stepper is improved as NA of lens systems becomes higher while the depth of focus becomes shallower. To simulate this phenomenon exactly, 3D exposure and development simulations were carried out by extending the Mack model to three dimensions. This extended model enables us to exactly simulate the asymmetrical change in the resist profiles with respect to defocus and to evaluate the focus latitude.

ACKNOWLEDGEMENTS

The author would like to thank Prof. Masataka Hirose and Prof. Mitsumasa Koyanagi at Research Center for Integrated Systems, Hiroshima University, for helpful discussion throughout this work.

REFERENCES

- [1] C.A.Mack, Understanding focus effects in submicrometer optical lithography, OPTICAL ENGINEERING, Vol.27, No.12, pp.1093-1100, 1988.
- [2] W.G.Oldham, S.Nandgaonkar, A.R.Neureuther, and M.O'Tool, A General simulator for VLSI lithography and etching process: Part-I application projection lithography, IEEE Tran., ED-26, pp.717-722, 1979.
- [3] A.Moniwa, T.Matsuzawa, T.Ito, and H.sunami, A Three-Dimensional Photoresist Imaging Process Simulator for Strong Standing-Wave Effect Environment, IEEE Tran., CAD-6, pp.431-437, 1987.

- [4] E.Barouch, B.Bradie, and S.V.Babu, Simulation of Three-Dimensional Positive Photoresist Images, *Jpn.J.Appl.Phys.*, Vol.28, No.12, pp.2624-2628, 1989.
- [5] F.Jones and J.Paraszczak, RD3D (Computer Simulation of Resist Development in Three Dimensions), *IEEE tran.*, ED-28, pp.1544-1552, 1981.
- [6] M.Fujinaga, N.Kokani, T.Kunikiyo, H.Oda, M.Shirahata, and Y.Akasaka, Three-Dimensional Topography Simulation Model: Etching and Lithography, *IEEE Tran.*, ED-37, pp.2183-2192, 1990.
- [7] E.W.Scheckler, K.K.H.Toh, D.M.Hoffstetter, and A.R.Neureuther, 3D Lithography, Etching, and Deposition Simulation (SAMPLE-3D), 1991 Symposium on VLSI Technology, pp.97-98, 1991.
- [8] Y.Hirai, S.Tomida, K.Ikeda, M.Sasago, M.Endo, S.Hayama, and N.Nomura, Three-Dimensional Resist Process Simulator PEACE (Photo and Electron Beam Lithography Analyzing Computer Engineering System), *IEEE Trans. on CAD*, Vol.10, No.6, pp.802-807, 1991.
- [9] T.Ishizuka, Three-Dimensional Simulation in Photoresist Development, *Trans. IEICE*, J73-C, No.11, pp.775-785, 1990 [in Japanese].
- [10] T.Ishizuka, *Computer Aided Innovation of New Materials*, Amsterdam, Elsevier, 1991, pp.735-739.
- [11] R.Dammel, C.R.Lindley, W.Meier, G.Pawlowski, J.Theis, and W.Henke, Consideration on the Focus Latitude for G-line and DUV Resists, *SPIE*, Vol.1264, pp.26-37, 1990.
- [12] M.Yeung, Modeling Aerial Images in Two and Three Dimensions, *Proc. Kodak Microelectronics Seminar INTERFACE '85*, pp.115-126, 1986.
- [13] F.H.Dill, A.R.Neureuther, J.Tuttle, and E.J.Walker, Modeling Projection Printing of Positive Photoresists, *IEEE Tran.*, ED-22, pp.456-464, 1975.

APPENDIX

One-dimensional solution of development time

It is a critical problem for accuracy of topography of resists to estimate the development time in a uniform gradient of development rate, because the development rates are calculated at discrete points, and linear interpolations are assumed in spatial development rates. The relation of surface position to development time is solved analytically in one-dimensional space with a uniform gradient development rate [9]. The development rates of position P_a and P_b are a and b , respectively. The distance between P_a and P_b is L . $v(t)$ and $x(t)$ are the functions of development rate and position with respect to development time t . The relationships are follows:

$$v(0) = a, \quad (17)$$

$$v(s) = b, \quad (18)$$

$$x(0) = 0, \quad (19)$$

Dimensional Positive
 4-2628, 1989.
 of Resist Development in
 and Y.Akasaka,
 and Lithography, IEEE
 reuther, 3D Lithography,
 mposium on VLSI
 a, and N.Nomura,
 and Electron Beam
 Trans. on CAD, Vol.10,
 Development, Trans.
 s, Amsterdam, Elsevier ,
 and W.Henke,
 sists, SPIE, Vol.1264,
 mensions, Proc. Kodak
 eling Projection Printing
 5.

$$x(s) = L, \tag{20}$$

where s is development time for L . The above notations and relationships are shown in Fig. 8. The uniform gradient in the space is expressed

$$dv/dx = \beta, \tag{21}$$

where $\beta = (b - a)/L$. Equation 21 is deformed with respect to time t :

$$dv/dt - \beta \cdot dx/dt = 0. \tag{22}$$

We solve eq. 22 under the conditions of eq. 17 to 20:

$$v(t) = a \cdot \exp(\beta \cdot t), \tag{23}$$

$$x(t) = (a/\beta) \cdot \{\exp(\beta \cdot t) - 1\}, \tag{24}$$

$$s = \ln(b/a)/\beta. \tag{25}$$

t time

to estimate the development
 development rates are
 umed in spacial
 ment time is solved
 development rate [9]. The
 vely. The distance between
 t rate and position with

- (17)
- (18)
- (19)

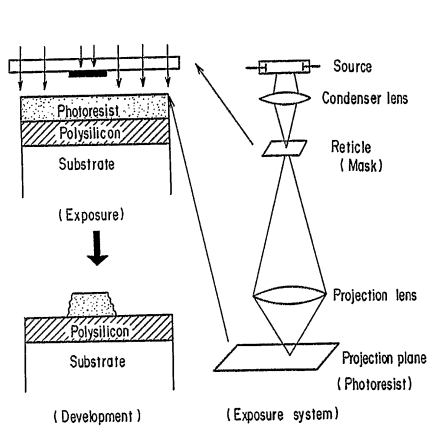


Fig. 1 Schematic diagram of optical projection printing system.

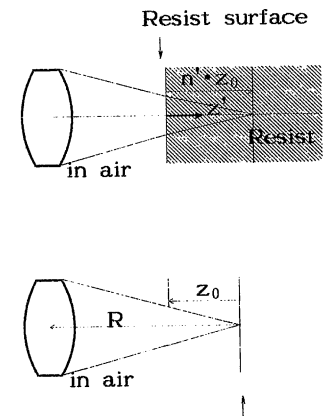
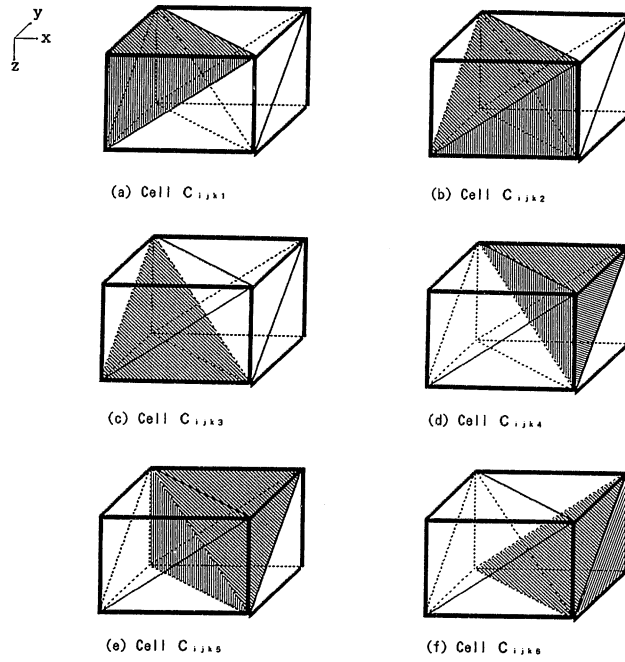
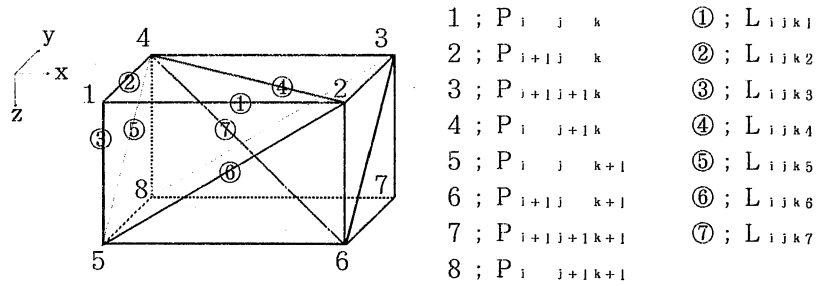


Fig. 2 A semi-finite refractive medium placed in image space.

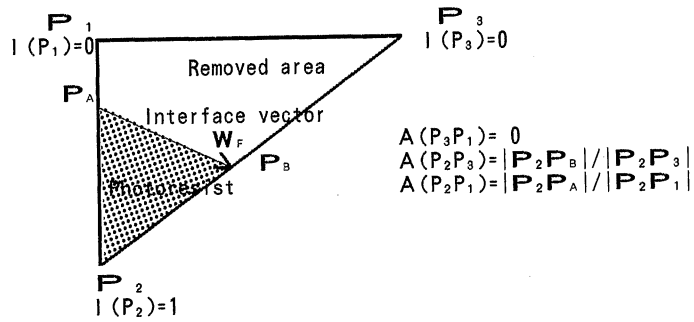


(a) Cell decomposition of the unit U_{ijk} .



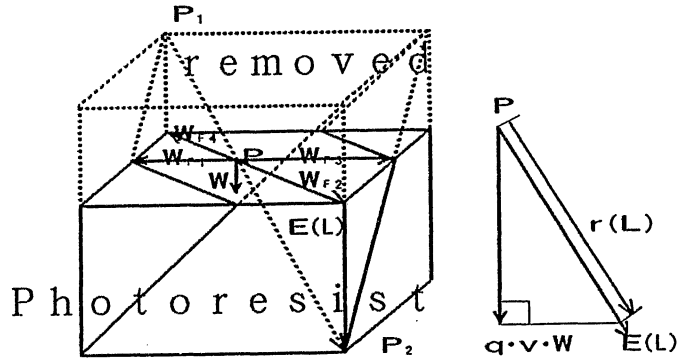
(b) Relationship of vertices and edges in the unit U_{ijk} . The numbers 1 to 8 are the vertices, and circled numbers 1 to 7 the edges.

Fig. 3 Cell decomposition and relationship of vertices and edges in the unit U_{ijk} .



\mathbf{P}_i : Position vector of the vertex P_i .
 $I(P_i)$: Development index.
 $A(P_iP_j)$: Development fraction of the edge line P_iP_j .

(a) Interface vector on the face of the tetrahedral cell.



(b) Development direction \mathbf{W} at \mathbf{P} calculated by interface vectors \mathbf{W}_{F_i} . (c) Development rate $r(L)$ at \mathbf{P} evaluated on the vector $\mathbf{E}(L)$.

$\mathbf{W}_{ij} = \mathbf{W}_{F_i} \times \mathbf{W}_{F_j}$: The normal vector of the surface spanned by \mathbf{W}_{F_i} and \mathbf{W}_{F_j} , where $ij=12, 23, 34, 41$.

$\mathbf{W} = \sum \mathbf{W}_{ij} / |\sum \mathbf{W}_{ij}|$: Development direction at \mathbf{P} .

$\mathbf{v} = \mathbf{v}(P_2) + \{\mathbf{v}(P_1) - \mathbf{v}(P_2)\} \cdot \mathbf{A}(L)$: Development rate of $\mathbf{P} = \mathbf{Q}(t)$.

$\mathbf{v}(P_i)$: Development rate of edge point P_i .

\mathbf{q} : parameter of fineness.

Fig. 4 Interface vectors and development directions.

- ① ; L_{ijk1}
- ② ; L_{ijk2}
- ③ ; L_{ijk3}
- ④ ; L_{ijk4}
- ⑤ ; L_{ijk5}
- ⑥ ; L_{ijk6}
- ⑦ ; L_{ijk7}

numbers 1 to 8 are the
 ges in the unit U_{ijk} .

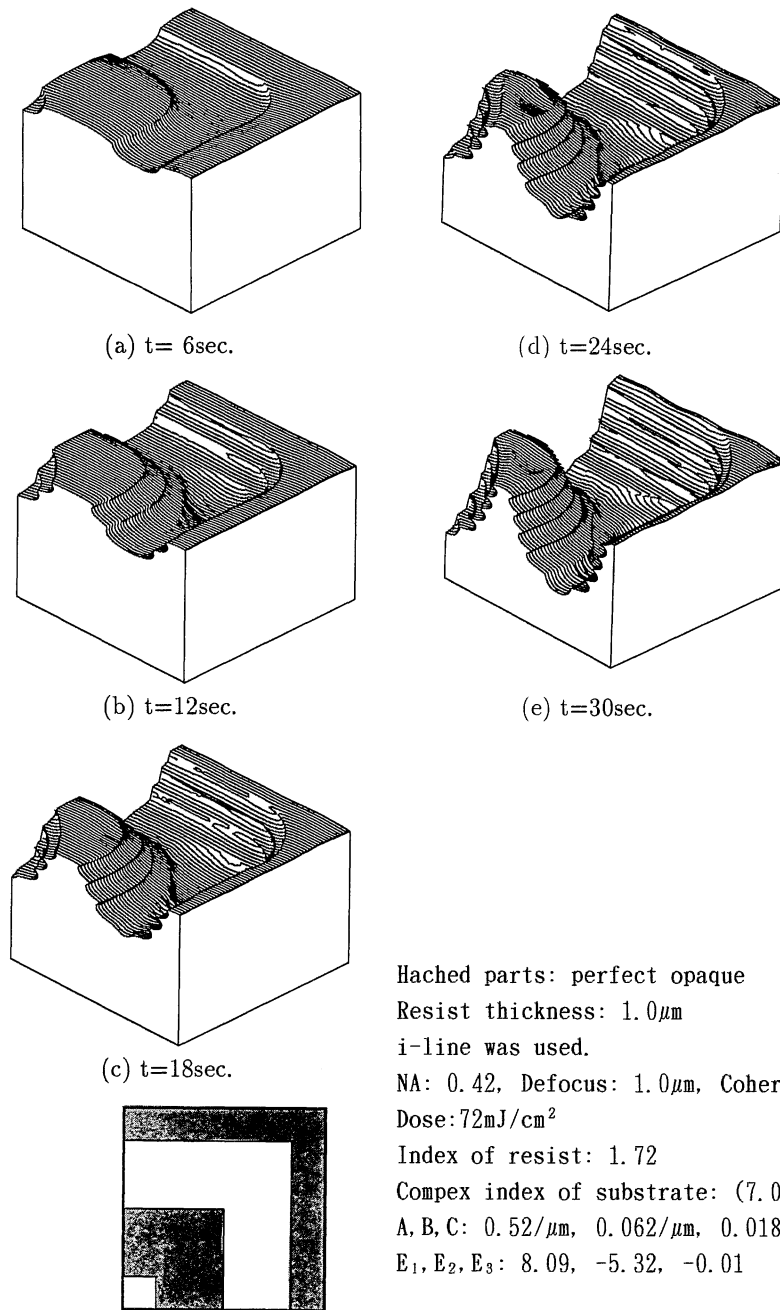


Fig. 5 Calculated photoresist profiles. t : development time. Decomposed number of units is $NX \cdot NY \cdot NZ=60 \times 60 \times 50$ and the parameter of fineness is 0.95.

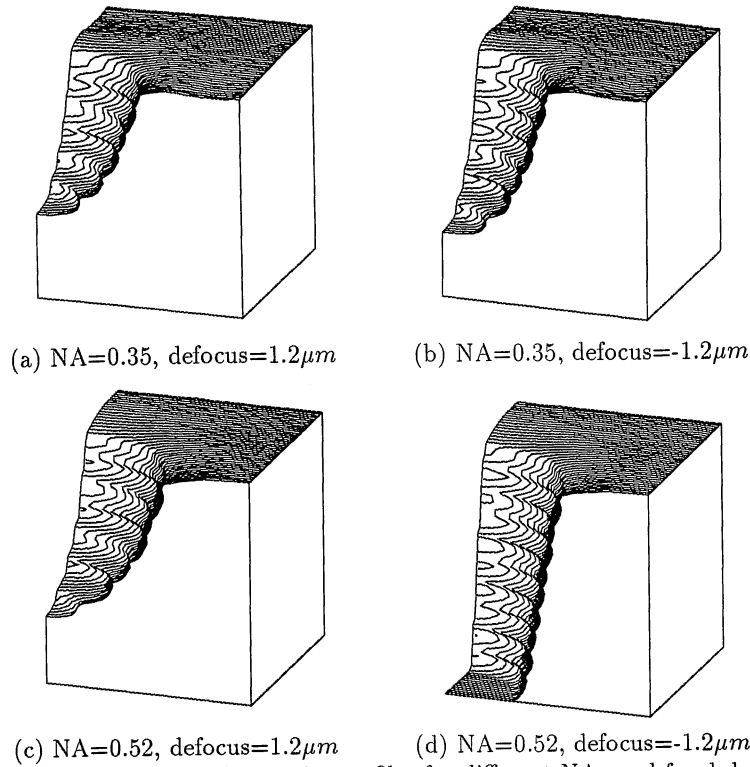


Fig. 6 Developed photoresist profiles for different NAs and focal depths.

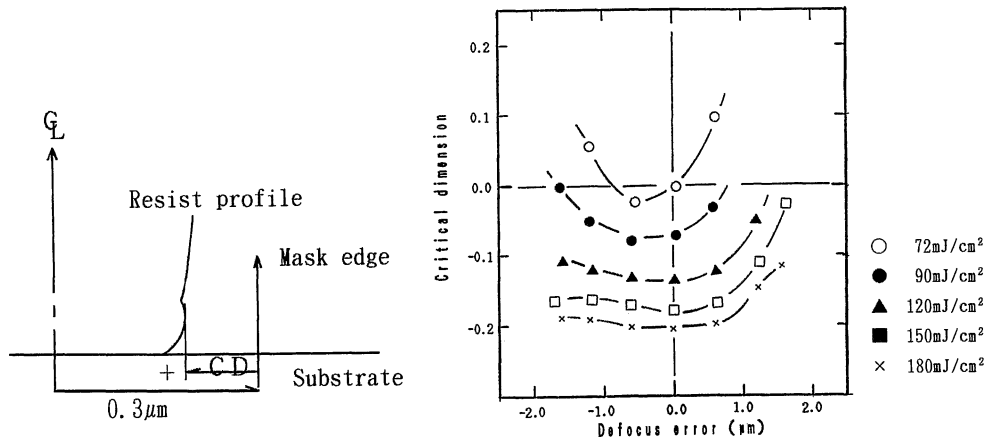
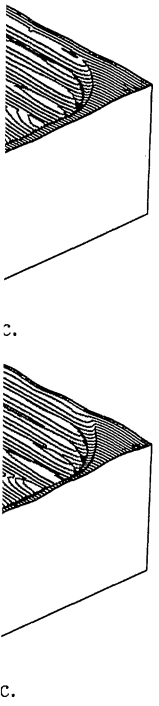


Fig. 7 Critical dimension vs focus.



ct opaque
0 μ m
1.0 μ m, Coherent factor: 0.5
72
strate: (7.0, -2.16)
2/ μ m, 0.018cm²/mJ
2, -0.01

. Decomposed number of
ness is 0.95.

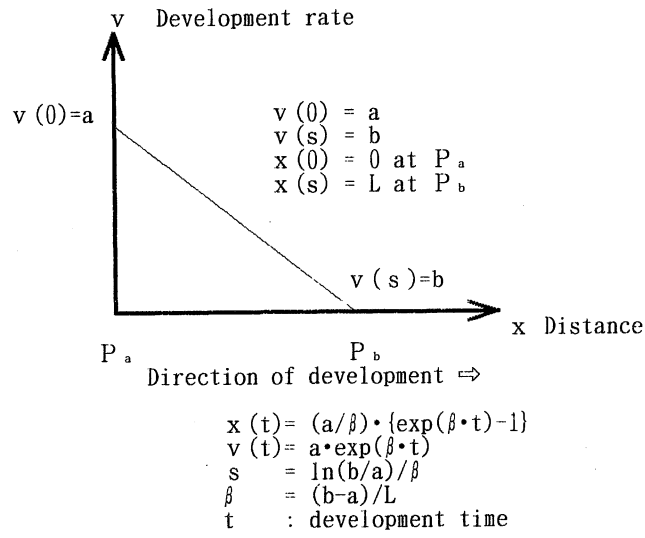


Fig. 8 Development rate in one-dimensional space.